SLAC-PUB-10557
July 2004

BEAM LOADING AND HIGHER-BAND LONGITUDINAL WAKES IN HIGH PHASE ADVANCE TRAVELING WAVE ACCELERATOR STRUCTURES FOR THE GLC/NLC*

R.M. Jones, V.A. Dolgashev, Z. Li, and T.O. Raubenheimer

*Stanford Linear Accelerator Center,
2575 Sand Hill Road, Menlo Park, CA, 94025

Abstract

A multi-bunch beam, traversing travelling wave accelerator structures, each with a $5\pi/6$ phase advance per cell, is accelerated at a frequency that is synchronous with the fundamental mode frequency. As per design, the main interaction occurs at the working frequency of 11.424 GHz. However, modes with frequencies surrounding the dominant accelerating mode are also excited and these give rise to additional modal components to the wakefield. Here, we consider the additional modes in the context of X-band accelerator structures for the GLC/NLC (Global Linear Collider/Next Linear Collider). Finite element simulations and field mode-matching models are employed in order to calculate the wakefield.

Paper presented at the 2004 9th European Particle Accelerator Conference (EPAC 2004)
Lucerne, Switzerland
5^{th} - 9^{th} July 2004

This work is supported by Department of Energy grant number DE-AC03-76SF00515*

BEAM LOADING AND HIGHER-BAND LONGITUDINAL WAKES IN HIGH PHASE ADVANCE TRAVELING WAVE ACCELERATOR STRUCTURES FOR THE GLC/NLC*

R.M. Jones, V.A. Dolgashev, Z. Li, and T.O. Raubenheimer; SLAC, USA

Abstract

A multi-bunch beam, traversing travelling wave accelerator structures, each with a 5π/6 phase advance per cell, is accelerated at a frequency that is synchronous with the fundamental mode frequency. As per design, the main interaction occurs at the working frequency of 11.424 GHz. However, modes with frequencies surrounding the dominant accelerating mode are also excited and these give rise to additional modal components to the wakefield. Here, we consider the additional modes in the context of X-band accelerator structures for the GLC/NLC (Global Linear Collider/Next Linear Collider). Finite element simulations and field mode-matching models are employed in order to calculate the wakefield.

INTRODUCTION

The main linacs of the 'warm' linear collider perform the task of accelerating the charged particle beam from an initial energy of 8 GeV to 250 GeV over a length of approximately 7 km. At a later date this will be upgraded to 500 GeV by increasing the active length of the linac [1]. The train of charged particles gains energy from the RF fields and consequently the beam modifies the fields. This modified electromagnetic field is known as the beam loaded field. In order to minimize the energy deviation along the train of bunches (each of which is separated from its neighbour by 1.4 ns) the profile of the unloaded accelerating gradient is carefully adjusted by changing the shape of the initial RF pulse that fills the structures. The beam loading compensation has been designed under the assumption that higher order monopole modes contribute little to the overall beam–loaded field profile. In this paper we investigate the actual perturbation that occurs due to higher order monopole modes by analysing these modes in the X-band accelerating structure known as H60VG3 [2]. This structure has an average fundamental mode group velocity of ~ 0.02c and a phase advance per cell of 5π/6.

We note the energy variation in an earlier X-band structure known as DDS (Damped and Detuned Structure) have been investigated using a low-pass filter to model the dispersive properties of the first monopole band [3]. This structure had an initial group velocity of 0.12c. Our present series of X-band structures has an initial group velocity of .03c and this is expected to give rise to larger dispersion in the energy profile. To analyse the modes in the accelerating structure, we employ two methods: firstly, a highly flexible finite element method generates the field within a single X-band structure and secondly, we use a mode matching method. The mode matching method is able to represent the effects of fundamental mode couplers loading down the structure.

This paper is organized in three main sections. The following section presents the results obtained using a 2-D finite element code. The section thereafter delineates the mode matching method and, the final main section addresses the implications of the higher order modes on beam-loading compensation.

FINITE ELEMENT CALCULATIONS

The overall electromagnetic fields in the structure are computed using the code 2-D code developed here at SLAC, *Omega2P* [4]. This code is sufficiently flexible such that it is able to faithfully represent detailed geometrical configurations in an accurate manner. The fields in the 55 cell X-band accelerator, known as H60VG3, are simulated with *Omega2P* including the fine details of the curvature of the cells. This code is used to calculate the eigen-modes of a closed structure.

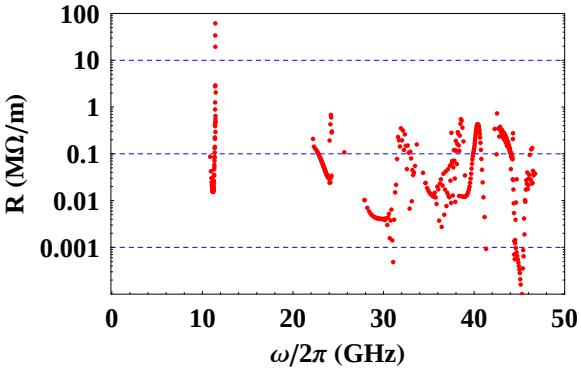

Figure 1: Shunt impedance of the longitudinal modes of the GLC/NLC 60 cm accelerating structure H60VG3. The mode frequency is shown along the abscissa.

Therefore, waveguide loading of the structure was not taken into account. This simulation required 11-fold parallel computing on a PC Pentium-4 cluster. The shunt impedance [4] of the accelerating mode is a measure of how efficiently the beam couples to the accelerating fields. This is illustrated in Fig. 1. The accelerating mode, at 11.424 GHz, has the largest shunt impedance (~62MΩ/m) of all modes. However, the modes in the first band – i.e. those above 10 GHz and below 12 GHz also have non-negligible values. The total longitudinal wakefield [5] is computed from the summation of the modes in the accelerating structure:

* Supported by the Department of Energy, grant number DE-AC03-76SF00515

$$W_{\parallel}(t) = 2\sum_{n=1}^{N_m} K_n \cos\omega_n t \exp\left(-\frac{\omega_n t}{2Q_n}\right). \quad (1)$$

Where, for the n-th mode: R_n is the shunt impedance, ω_n the angular frequency, Q_n is the quality factor and K_n ($=\omega_n R_n/4Q_n$) is the loss factor. Also, t is the time recorded from the first accelerated bunch of charged particles and N_m is the total number of longitudinal modes.

If we multiply the longitudinal wake in (1) by the charge of a single bunch ($1.6\text{x}10^{-19}\text{x}0.75\text{x}10^{10}$ Coulombs) then we obtain the wake potential per unit length. The amount that the higher order modes contribute to this longitudinal wake potential is illustrated in fig 2. We calculated the sum wakefield [6] for the higher bands and its standard deviation is ~0.13%. With suitable beam loading compensation we expect that this can be significantly reduced.

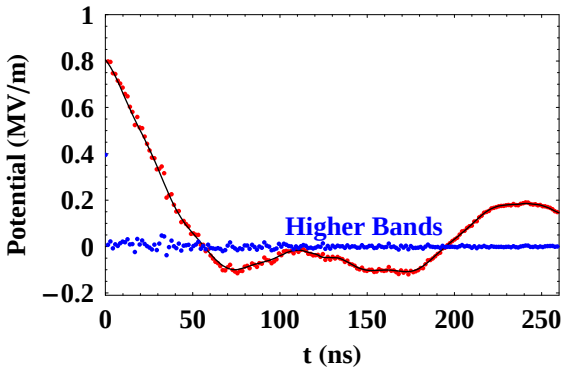

Figure 2: Longitudinal potential evaluated at the location of each bunch versus time. The potential due to the complete wake, first band wake and higher order band wake is given by red dots, a sold line and blue dots, respectively.

This calculation of the shunt impedance and mode frequencies is limited by the fact that the reflections that occur at the fundamental mode coupler are not taken into account. To overcome this limitation initially we calculate the first band using a mode matching method. Using the results of this calculation we investigate beam loading compensation.

MODE MATCHING METHOD

We use the mode matching method [7] to obtain the fields in the structure matched to the fundamental coupler within a limited bandwidth. This method is readily extendable to higher order bands. Here we investigate the beam loading and energy compensation for the first band. In future studies we will consider higher bands.

In order to minimize the computational time we approximate all geometrical transitions to sharp changes in cross-section. Thus, irises become rectangular corners, as is natural to the mode matching method.

The objective of the whole simulation will be to obtain the beam loaded gradient. In order to proceed towards this objective we are first required to parameterize the 60 cm X-band accelerator structure. To this end, we take 5 fiducial cells from the structure, subject them to periodic boundary conditions and using the code *Omega2P*, obtain the mode frequencies for the zero and π phase for each cell. Subsequently we obtain the frequencies for all other cells by cubic spline nterpolation. The results of the zero and π phase advance frequencies

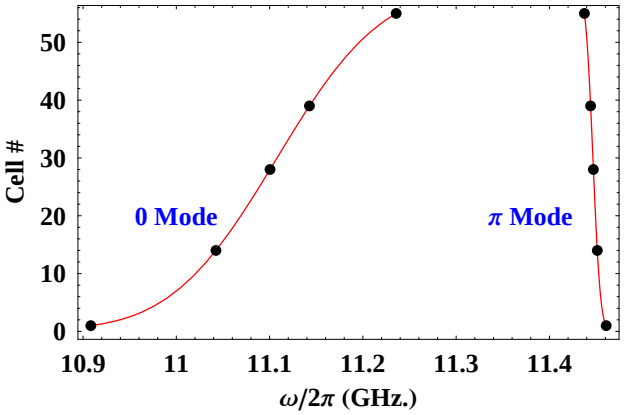

Figure 3: Cell frequencies for zero and π phase advance. The dots are all computed with *Omeaa2P*

are illustrated in Fig. 3. Utilizing the mode matching code *Smart-2D* [8] for a single iris and cavity subjected to periodic boundary conditions we vary the iris radius and the cavity radius until all the 0 and π frequencies are obtained. Armed with these parameters, we then cascade the S-matrices of each individual transition to obtain the S-matrix of the overall structure.

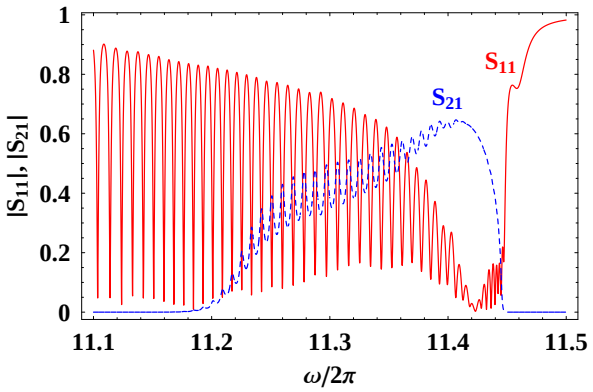

Figure 4 Input reflection (S_{11}) and transmission (S_{21}) of accelerating structure.

We match-out the structure over the band of the accelerating mode, by varying the cavity radius and iris radius of the input and output accelerator cells. This models the effect of the reflective properties of the fundamental mode couplers quite adequately. The reflection and transmission properties of the structure obtained from this simulation are shown in Fig. 4. We note that the couplers are well-matched at the accelerating frequency as the reflection coefficient is no more than

0.02 at 11.424 GHz. Also, Ohmic copper losses are included in the simulation. For this reason we expect the overall S-matrix to be non-unitary (Fig. 4).

In order to assess the influence of higher order mode beam-loading we calculate the beam impedance over the band of the accelerating frequency using the mode matching code *Smart-2D* once more. The result of this calculation is illustrated in Fig. 5. As expected, this impedance is peaked at the accelerating frequency.

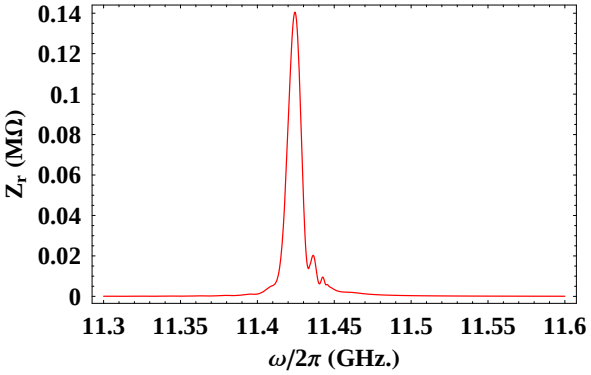

Figure 5: Real part of longitudinal beam impedance

The higher frequency modes of the first band are revealed in the shoulder of the resonant peak (in the region of 11.44 GHz). Also, it is worth noting that the integral of the impedance over all frequencies gives the total loss factor as 1.765 V/pC/m which is in good agreement with 1.763 V/pC/m, as simulated with *Omega2P*.

From these calculations we are able to obtain the total beam-loaded accelerating gradient and this is discussed in the following section.

INFLUENCE OF DISPERSION ON BEAM LOADING

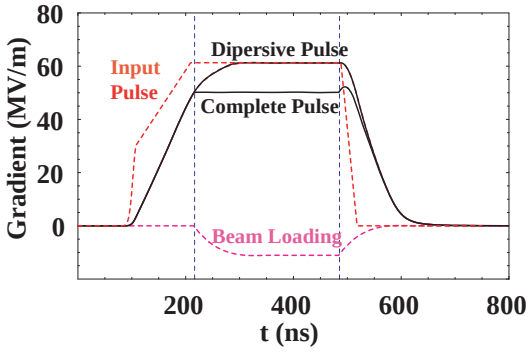

Figure 6: Input pulse (red), complete pulse and its components: beam loading (magenta), dispersive pulse. The vertical (dashed and blue) lines indicate the duration of the train of accelerated bunches.

The impedance function enables the beam-loading gradient to be calculated and, adding the initial pulse which is propagated down the structure we are able to obtain the total beam-loaded gradient. The results of this calculation with a ramped flat-top input pulse are illustrated in Fig. 6. The energy deviation at the final focus for the GLC/NLC is required to have an RMS value of no more than 0.25% [9]. The energy deviation along the bunch train and its beam loading component are illustrated in Fig. 7. Note that the deviation of initial part

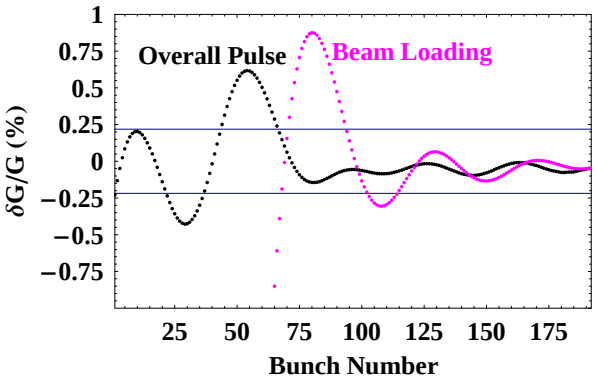

Figure 7: Percentage energy deviation along pulse train.

of the beam loading component is larger than 1%. The RMS of the total energy deviation of the pulse train is ~0.25%. By tailoring the amplitude profile of the input RF pulse, this energy deviation is readily reduced to 0.13% [10].

Thus, in conclusion the first band longitudinal modes do perturb the longitudinal beam loading profile but their effect can be minimized by tailoring the input RF pulse appropriately. In practice the phase and amplitude of the klystrons which supply the power can be carefully varied to produce the desired pulse amplitude profile [11].

REFERENCES

[1] International Linear Collider Technical Review Committee, Second Report, SLAC-R-606, 2003.
[2] R.M. Jones *et al.*, PAC03, SLAC-PUB-9868, 2003.
[3] K.A. Thompson and R.D. Ruth, PAC93, SLAC-PUB-6154., 1993
[4] X. Zhan, Parallel Electromagnetic Field Solvers Using Finite element Method with Adaptive Refinement and Their Application To Wakefield Computation of Axisymmetric Accelerator Ph.D. thesis, Stanford University, 1997.
[5] P.B. Wilson, Introduction to Wakefields and Wake Potentials, SLAC-PUB-4547, 1989.
[6] R..M. Jones *et al.*, PAC99, SLAC-PUB-8101, 1999
[7] T. Itoh, Numerical Techniques for Microwave and Millimeter-Wave Passive Structures, 1989 (John Wiley and Sons, pub.).
[8] V.A. Dolgashev, ICAP 98, Monterey, CA, 1998.
[9] P. Tenenbaum, private communication, 2003.
[10] R.M. Jones, *et al.*, PAC03, SLAC-PUB-9870, 2003
[11] S.G. Tantawi *et al.*, submitted to Physical Review STAB, SLAC-PUB-10520, 2004.